Modeling soil water dynamics considering measurement uncertainty

Isaya Kisekka, K. W. Migliaccio, R. Muñoz-Carpena, B. Schaffer and Y. Khare

Published Version Information

Citation: Kisekka, I., Migliaccio, K. W., Muñoz-Carpena, R., Schaffer, B., & Khare, Y. (2015). Modelling soil water dynamics considering measurement uncertainty. Hydrological Processes 29(5), 692-711.

Digital Object Identifier (DOI): doi:10.1002/hyp.10173

Publisher's Link: http://onlinelibrary.wiley.com/doi/10.1002/hyp.10173/abstract

Modeling Soil Water Dynamics Considering Measurement Uncertainty

Isaya Kisekka[1,2], K.W. Migliaccio[2], R. Muñoz-Carpena[3], B. Schaffer[2], and Y. Khare[3]

[1] Kansas State University, Southwest Research-Extension Center, 4500 E. Mary St., Garden City, KS 67846, E-mail: ikisekka@ksu.edu

[2]University of Florida, IFAS Tropical Research and Education Center 18905 SW 280th St Homestead, FL 33031, klwhite@ufl.edu , bas56@ufl.edu

[3]University of Florida, Agricultural and Biological Engineering Department, P. O. Box 110570, Gainesville, FL 32611, carpena@ufl.edu , khareyogesh1@ufl.edu

Corresponding author: Isaya Kisekka, Kansas State University, Southwest Research-Extension Center, 4500 E. Mary St., Garden City, KS 67846, E-mail: ikisekka@ksu.edu

Abstract

In shallow water table controlled environments, surface water management impacts groundwater table levels and soil water dynamics. The study goal was to simulate soil water dynamics in response to canal stage raises considering uncertainty in measured soil water content. WAVE (Water and Agrochemicals in the soil, crop and Vadose Environment) was applied to simulate unsaturated flow above a shallow aquifer. Global sensitivity analysis was performed to identify model input factors with greatest influence on predicted soil water content. Nash-Sutcliffe increased and Root Mean Square Error reduced when uncertainties in measured data were considered in goodness-of-fit calculations using measurement probability distributions and probable asymmetric error boundaries; implying that appropriate model performance evaluation should be done using uncertainty ranges instead of single values. Although uncertainty in the experimental measured data limited evaluation of the absolute predictions by the model, WAVE was found a useful exploratory tool for estimating temporal variation in soil water content. Visual analysis of soil water content time series under proposed changes in canal stage management indicated that sites with land surface elevation of less than 2.0 m NGVD29 were predicted to periodically experience saturated conditions in the root zone and shortening of the growing season if canal stage is raised more than 9 cm and maintained at this level. The models developed could be combined with high resolution digital elevation models in future studies to identify areas with the greatest risk of experiencing saturated root zone. The study also highlighted the need to incorporate measurement uncertainty when evaluating performance of unsaturated flow models.

Key words; Soil water, measurement uncertainty, vadose zone, WAVE, root zone saturation

Introduction

In shallow water table controlled environments, regional surface water management operations impact groundwater table levels which in turn affect soil water dynamics. An example is the operational adjustments in surface water management that are occurring in south Florida as part of an effort to restore the hydrology of Everglades National Park (ENP)(USACE and SFWMD, 2011). Rises in water table due to proposed rises in canal stage could affect soil water content in agricultural fields adjacent to ENP through transient root zone saturation. Negative impacts of a saturated root zone on plants including reduced yield and physiological function are well documented in literature (Lizaso and Ritchie, 1997; Schaffer, 1998).

In addition, rises in shallow water table could increase risk of temporary groundwater flooding due to rapid water table responses to storm events. Earlier studies have observed disproportionate rises in water table elevations after intense rainfall (Kayane and Kaihotsu, 1988; Waswa *et al.* 2013). Germann and Levy (1986) attributed the rapid rise in water table elevation in response to precipitation to capillary fringe groundwater ridging in which a small addition of water to the capillary fringe resulted in a rapid and large rise in water table elevation that drops immediately after the storm.

One way of assessing potential impacts of surface water management decisions on soil water dynamics is through monitoring and modeling. A normally preferred approach is the use of process models. The main advantage of process-based vadose zone models over statistical or empirical models such as that used in Kisekka *et al.* (2013c) is they are transferable. Several vadose zone models are available, such as WAVE (Water and Agrochemicals in the soil, crop and Vadose Environment), HYDRUS, and SWAP (Soil-Water-Atmosphere-Plant). These models typically predict water, heat and solute movement in the unsaturated zone.

To adequately characterize vadose models and enhance their proper use, model uncertainty as well as uncertainty in measured soil water data used in model parameterization and evaluation needs to be considered. There are many sources of uncertainty which make soil water content measured by indirect soil water monitoring methods (e.g., time domain reflectometer [TDR], and capacitance sensors) uncertain. Sources of uncertainty include 1) errors related to equipment installation and calibration, 2) errors associated with the measurement technique and algorithms that are used to convert surrogate measurements to soil water content, and 3) errors associated with spatial variability of soil properties (IAIA, 2008). For example, uncertainty in TDR measurements can mostly be attributed to effects of soil electrical conductivity and dielectric relaxation on the calibration equation (Lin, 2003). Errors in soil water measurements by capacitance sensors can be attributed to small scale variations in soil water content due to the small volume of soil sensed, temperature and soil bulk electrical conductivity (Evett et al. 2012). Errors may be random or systematic. Random errors maybe minimized through proper sampling and calibration but other types of errors are beyond the control of the user of the soil water monitoring equipment and these become a source of systematic uncertainty in measured soil water data (e.g., non-uniform distribution of the electromagnetic field of capacitance probes around the access tube which results in overestimation of soil water).

In many soil water prediction model performance evaluations (Whiting *et al*., 2004; Merdun *et al*., 2006; Chen *et al*., 2012; Ritter and Muñoz-Carpena, 2013) Goodness-of-fit indicators such as Nash-Sutcliffe (NSE), Willmot index (d), Root Mean Square Error (RMSE), and Mean Absolute Error (MAE) are used. These goodness-of-fit indicators are usually based on calculating the pairwise error between observed and predicted soil water content without accounting for the uncertainty in measured data. Accurate evaluation of model performance needs to consider this source of uncertainty whenever possible in order to provide a more realistic assessment of model performance and to provide guidance for model output interpretation (Harmel et al., 2010). Bilskie (2001) describes a simple statistical procedure to quantify uncertainty due to spatial variability in soil water content but does not cover uncertainty due to instrumentation. Harmel and Smith (2007) provide a framework for quantifying uncertainty in measured data, while Harmel *et al*. (2010) outlines a procedure for quantifying model uncertainty for models in which the predicted state variable can be assumed independent. The later approach may need modification for soil water simulations because soil water content cannot be assumed independent due to autocorrelation. Another approach that has been used to address measurement uncertainty in hydrologic model inputs include use of the Bayesian total error analysis methodology (Kavetski *et al.* 2006), but this approach tends to be computationally intensive.

The study goal was to simulate soil water dynamics in response to surface water management in the C-111 basin of Florida considering measurement uncertainty. The objectives were to: (1) apply the vadose zone model WAVE for simulating soil and limestone bedrock water content dynamics at four sites monitored, (2) evaluate model performance considering uncertainty in measured soil and limestone bedrock water content, and (3) apply the models to investigate the effect of 6, 9 and 12 cm incremental rises in canal stage on soil and limestone bedrock water dynamics at 10, 20, 30 and 40 cm monitoring depths.

Material and methods

Study area and experimental set up

The study was conducted in Miami-Dade County close to Homestead, Florida, within an agricultural area approximately 17 km^2 (Figure 1) immediately to the east of canal C-111. Topography is essentially flat, implying that the assumption of 1D vertical flow for the unsaturated zone is valid. Soil depth is shallow ranging between 10 and 25 cm. The limestone bedrock layer is highly porous and reached on average at 20 cm depth.

Two multi-sensor capacitance probes (EnviroScan probes, Sentek Technologies, Ltd., Stepney, Australia) for soil water monitoring were installed at four locations (Figure 1) at distances of 500, 1000 and 2000 m from the canal. Each probe had four sensors positioned at 10, 20, 30 and 40 cm from the ground surface (Figure 2). Soil water content was recorded every 15 minutes and averaged daily. A detailed description of EnviroScan operation can be found in Kisekka *et al*. (2013c). The top 20 cm typically represented the scarified soil layer which is used for crop production and the lower 20 cm represented the underlying limestone bedrock in which plant roots cannot penetrate.

Calibration of capacitance sensors in the field using the standard gravimetric sampling approach (Sentek Pty Ltd, 2001) was attempted but later abandoned due to several factors including: 1) difficulty obtaining soil samples adjacent to the sensor access tube without interfering with the operation of the sensors; 2) difficulty in obtaining a wide range of soil water content under field conditions to properly calibrate the sensors; and 3) presence of a shallow limestone bedrock in which it was difficult to sample. Evett et al. (2012) noted that field calibration may not resolve the issue of accuracy associated with capacitance type soil water sensors. This was attributed to the high sensitivity of the sensors to soil bulk electrical conductivity and temperature, non-uniform distribution of the electromagnetic field around the plastic access tubes, and changes in soil structure over time and space. However, Gabriel et al. (2010) compared default and calibrated volumetric soil water content from EnviroScan sensors in a field study and concluded that although the sensors tend to over-estimate water content, the sensors were accurate in reproducing soil water dynamics. Thus, the value of capacitance probes in the present study was their ability to respond well to dynamics of soil water content (Evett, 2000).

Numerical modeling of unsaturated flow with WAVE

A vadose zone computer code called WAVE developed by Vanclooster *et al*. (1995) that solves the one dimensional (1D) Richards' equation using finite difference techniques was applied. WAVE simulates the transport of water, energy, non-reactive solutes, nitrogen, and pesticides in the soil-crop continuum.

Simulated system depth varied between 200 and 220 cm to account for the variations in depth to the water table at the different locations. The soil profile was discretized into 5 cm compartments and a numerical solution was obtained at the center of each of the compartment (Figure2).

The minimum and maximum time steps were set to 0.01 and 1 day, respectively. The initial condition was obtained by assuming drain to equilibrium conditions within the soil profile.

In WAVE, unsaturated flow is simulated using *h*-based formulation of Richards' equation:

$$C(h)\frac{\partial h}{\partial t} = \frac{\partial}{\partial z}\left[K(h)\left[\frac{\partial h}{\partial z}+1\right]\right] - S(z,h) \qquad (1)$$

where *C(h)* is the differential moisture capacity [L^{-1}], equal to the slope of the soil water retention curve; *h* is the soil water pressure head [L]; *t* is the time [T]; *z* is the vertical space coordinate; and *K(h)* is unsaturated hydraulic conductivity. The van Genuchten–Mualem models was used to calculate *K(h)* in this study (Eqs. 2 and 3; Mualem, 1976 and van Genuchten, 1980):

$$\theta(h) = \begin{cases} \theta_r + \dfrac{\theta_s - \theta_r}{[1+|\alpha h|^n]^{(1-1/n)}} & h < 0 \\ \theta_s & h > 0 \end{cases} \qquad (2)$$

$$K(h) = Ksat * S_e^{\lambda}\left[1-(1-S_e^{1/(1-1/n)})^{(1-1/n)}\right]^2 \qquad (3)$$

where θ_r and θ_s are residual and saturated soil water content respectively, α is inverse of the air entry value, *n* is pore size distribution index, *Ksat* is saturated hydraulic conductivity, *Se* effective saturation (normalized volumetric water content θ) and λ is pore connectivity. The parameters of the van Genuchten equation for layer 1 were estimated in the laboratory using measurements of suction and volumetric water contents collected using Tempe cells and Richards's pressure plate and then fitted the retention curve using RETC tool (van Genuchten, 1991). Soil water retention characteristics for layer 2 were not directly measured due to difficulty in obtaining undisturbed samples from the limestone bedrock and the extremely porous nature of the material. Saturated water content for the limestone bedrock was estimated when the sensors at 30 and 40 cm were below the water table. Initial literature values for the other retention curve parameters for layer 2 i.e., θ_r and parameters *n* and α were obtained from literature (Muñoz-Carpena *et al*., 2008). Initial pore connectivity parameter (λ) values were obtained from literature (Mualem, 1976) but were assumed to vary between 0.5 and 1.5.

The sink term *S(z,h)* was expressed as a function of the maximum root water uptake (S_{max}) as proposed by Feddes *et al*. (1978) which is a function of *z*. In this study, a linear relationship was assumed for S_{max} and the parameters *A* and *B* in Eq. 4 were obtained by specifying S_{max} at different compartments to range between 0.001 and 0.012 (Vanclooster *et al*., 1996). A dimensionless reduction function *α(h)* ranged between 0 and 1 as described in Vanclooster *et al*., 1996.

$$S(z,h) = \alpha(h)\, S_{\max} = \alpha(h)\left[A - Bz\right] \qquad (4)$$

We simulated root water uptake by describing a Leaf Areas Index (LAI), root growth depth, and crop coefficient (Kc) time series for sweet corn as it represented a dominant crop grown at the study site. Crop evapotranspiration (ET_{crop}) was partitioned into potential soil evaporation (*Ep*) and potential transpiration (T_p) following Ritchie (1972):

$$E_P = e^{-c*LAI} * ET_{crop} \qquad (5)$$

$$T_P = ET_{crop} - E_P - \frac{CanStor}{1day} \quad (6)$$

where *c* is the radiation extinction coefficient was set to 0.6 (Vanclooster *et al*. 1995), CanStor representing the amount of water intercepted and released from the canopy (mm) was assumed negligible and considered to be zero for computational purposes, ET_{crop} is calculated as a product of reference evapotranspiration and a crop coefficient, other terms in Eqs. 5 and 6 are described as before. Meteorological data for calculating reference evapotranspiration were obtained from the Florida Automated Weather Network station located 10 km north of the study site. LAI for sweet corn was measured using a LI-3100C Area Meter (LI-COR, Inc, Lincoln, Nebraska USA). Kc values for sweet corn grown in south Florida were obtained from Muñoz-Carpena *et al*. (2008).

A groundwater table boundary condition was used as the bottom boundary as study motivation was in part to investigate the impact of the raised water table on soil water dynamics. The time series of water table depth were simulated using MODFLOW as described in Kisekka *et al.* (2013b). The boundary condition at the top was a flux calculated as:

$$K(h)\left[\frac{\partial h}{\partial z}+1\right] = -Q_S = -\left[E_{pot} - \left(Rain + Irr + \frac{Pond - Intc}{\Delta t}\right)\right] \quad z = 0 \quad (7)$$

where Q_s is the potential flux through the soil surface (cm/day) defined positive upwards, E_{pot} is potential soil evaporation, *Rain* is precipitation (cm/day), *Irr* is irrigation (cm/day), *Pond* is ponding depth at surface (cm), and *Intc* is storage capacity of the canopy (m). *Irr, Pond*, and *Intc* were not measured and for computational purposes were assigned values of zero. We acknowledge that having information on irrigation applications especially in the growing season (November to May) would have improved our model representation of the real physical system but the study was conducted on commercial production farms where irrigation application were not metered.

Calibration, sensitivity analysis and model validation of WAVE

To avoid over fitting the model to uncertain data, we did not use parameter estimation techniques that seek to minimize the difference between measured and predicted value. Instead calibration was completed by adjusting parameter values within ranges established through measurement or literature until the fit between simulated and measured soil water content was acceptable (within the uncertainty range of measured data). The length of soil water content time series at each site varied due to differences in the dates of installation of the capacitance probes and also due to malfunction and replacement of sensors at different sites during the study (Table 1). For each site half of the data was used for model calibration and the remaining half for model validation.

Global sensitivity analysis was implemented in two stages (Saltelli et al., 2004; Muñoz-Carpena et al., 2007). First the improved Morris method by Campologo *et al*. (2007) was applied to obtain qualitative ranking of parameters and then using a subset of critical parameters from step 1, Sobol' analysis was performed to determine quantitative first order and total effects sensitivity indices. Parameters included in sensitivity analysis for layers 1 and 2 at different sites are given in Table 2. For all the parameters with the exception of LAI and Kc, a uniform distribution was assumed and parameters ranges were obtained from measurements or literature. To test the sensitivity of simulated volumetric soil water content to variations in LAI, a discrete uniform distribution was assumed using three values representing LAI during initial plant development stage, mid-season stage, and late season stage. LAI values are based on measurements collected in a sweet corn field during the study (Table 3). A similar approach was used for testing sensitivity of simulated volumetric water content to variations in Kc.

Campologo *et al*. (2007) sensitivity analysis was implemented using Matlab algorithms (R2012a , Mathworks Inc., Natick, Massachusetts) developed by Saltelli *et al*. (2008) (http://sensitivityanalysis.jrc.it/software/index.htm). Matlab was used to automatically execute WAVE for each parameter set in the generated sample input file. For sample generation using Campolongo *et al*. (2007) method, the following settings were used: number of levels (p) was 4, size of oversampling (N) was 1000, number of trajectories (r) was 20, and number of parameters (k) was 19. This resulted in a total of 400 parameter sample sets (i.e., $r(k+1)=400$). The number of WAVE executions for Sobol analysis was estimated as $2n(k+1)$, where the sample size, n was 512 and k is the number of critical parameters identified from Campologo *et al*. (2007) analysis. Nash-Sutcliffe coefficient (NSE) and the Root Mean Square Error (RMSE) were calculated as the model output for each simulation.

Estimating uncertainty in measured soil and bed rock water content

To account for error sources, we quantified uncertainty for each measured soil and bedrock water content value. Uncertainty in measured soil and bedrock water content data was accounted for using a correction factor based on an assumed probability distribution for each measurement (Harmel and Smith, 2007; Harmel *et al*., 2010). The correction factor modifies the error term (i.e., the pair-wise difference between measured and predicted values) in goodness-of-fit indicators by incorporating the distribution of the measurement uncertainty as shown:

$$e(measured)_i = \frac{CF(measured)_i}{0.5}(O_i - P_i) \quad (8)$$

where $e(measured)_i$ is the modified deviation between measured and predicted soil water content for point i considering only measurement uncertainty, $CF(measured)_i$ is the non-dimensional correction factor (ranges between 0 and 1) for each measured soil and bedrock water content (O_i) and predicted soil and bedrock water content (P_i) considering measurement uncertainty, and 0.5 refers to one sided probability for (O_i) at mean value assuming a symmetric distribution.

WAVE was calibrated by manually adjusting parameter values within the ranges in Table 2. These ranges were selected based on laboratory measurements or literature and represented the range in values for each parameter. Thus, these ranges were the best estimate of parameter distribution. Parameter values were adjusted until the simulated soil water content was within the maximum and minimum uncertainty bounds of the measured data and calculated as:

$$\alpha = \bar{x} - \sqrt{3}\,\bar{x}Cv \tag{9}$$

$$\beta = \bar{x} + \sqrt{3}\,\bar{x}Cv \tag{10}$$

where the uncertainty bounds α and β are the lower and upper bounds of the uniform distribution, $\bar{x}$ is the mean of the distribution for measurement i set at the measured value and Cv is coefficient of variation (Harmel *et al.*, 2010). We assumed a uniform distribution for all measurements and minor (Cv=0.02) to moderate (Cv=0.08) uncertainty depending on how variable the data collected from two adjacent capacitance probes was. However, this method assumes a symmetric distribution which may deviate from the true distribution for each measurement.

Since probability distribution of measured soil water can be asymmetric, to account for asymmetry corresponding to each measurement, we used the probable error range (PER) approach for modifying the error between observed and predicted values described by Harmel and Smith (2007). This approach does not require knowing the probability distribution of the measurements, it involves the use of PER in measurement based on professional judgment or literature. We set a probable uncertainty lower boundary length of 5% of the measured value and an upper boundary length of 2.5% of the measured value based on average deviations of measured values from long term average soil water content during the study period. In this approach the deviation between the predicted and measured values for each corresponding pair for calculating Goodness-of-fit is modified based on whether the predicted value falls within the uncertainty range of the corresponding measured value or outside the uncertainty range as shown in equations 11 and 12 (Harmel and Smith, 2007)

$$UO_i(u) = O_i + \frac{PER_{iu} * O_i}{100}, \quad UO_i(l) = O_i - \frac{PER_{il} * O_i}{100} \tag{11}$$

$$Modified\,(O_i - P_i) = \begin{cases} 0, & UO_i(l) \le P_i \le UO_i(u) \\ UO_i(l) - P_i, & P_i < UO_i(l) \\ UO_i(u) - P_i, & P_i > UO_i(l) \end{cases} \tag{12}$$

were $UO_i(u)$ is the upper uncertainty boundary, $UO_i(l)$ is the lower uncertainty boundary, PER_{iu} is the upper probable error range for each measured data point, PER_{iu} is the lower probable error range for each measured data point, O_i and P_i are described as previously.

After calibration, model performance (validation) was assessed using the procedure described by Ritter and Muñoz-Carpena (2013) which determines the statistical significance of Goodness-of-fit indicators. The methodology is implemented by the computer program FITEVAL. Ritter and Muñoz-Carpena (2013) use the bootstrapping technique described by Politis and Romano (1994) to derive approximate probability distributions for the NSE and RMSE Goodness-of-fit indicators. The derived probability distribution is then used in a hypothesis testing of the Goodness-of-fit exceeding a threshold value ($NSE_{threshold}$=0.65 is used in this study). The null hypotheses (*H0*) denotes that the median $NSE < NSE_{threshold}$ (model performance is not acceptable) while the alternative hypotheses (*H1*) denotes that the median $NSE \geq NSE_{threshold}$ (model is acceptable). The null hypothesis is rejected and alternative accepted when the *p-value* is below the significance level α which can be 0.01, 0.05, or 0.1. The *p-value* represents the probability of wrongly accepting the model fit when it should have been rejected (i.e., *H0* is true). The probability distribution is also used for computing the probability of the *NSE* being within a given range. Using FITEVAL, validation was performed in two stages: 1) without considering uncertainty in measured values and 2) accounting for uncertainty in measured values following procedures described in Harmel *et al*. (2010) and in Harmel and Smith (2007).

Model applications

The validated models at each of the four sites were applied to simulate soil and limestone bedrock water content at different depths under 6, 9 and 12 cm incremental raises in canal stage. Effect of surface water management on water table elevation was simulated using MODFLOW as described in Kisekka *et al.* (2013c). The simulated water table elevation was then used as a lower boundary condition of the WAVE soil profile, which allowed us to simulate the effect of the proposed changes in surface water management on soil water dynamics in the agricultural fields.

Results and discussion

Sensitivity analysis and calibration

Due to brevity, only Morris results for site 4 (the closest site to the canal; Figure 1) are presented (Table 4). Values for the other sites were within the ranges of site 4; it is also worth noting that parameter ranking at all sites was similar. The magnitudes of the Morris sensitivity measures μ* (which assesses the overall effect of the factor on model output) and σ (which indicates effects of a factor's interactions with other factors) were greater for parameters of the van Genuchten equation, i.e., θ_r and θ_s, α and n (Tables 4). This indicates that the predicted soil and limestone bedrock water contents were more sensitive to soil hydraulic properties than vegetation cover. This would be expected because soil water retention curve parameters characterize soil water retention in both soil and limestone bedrock layers (Muñoz-Carpena *et al*., 2008). *Ksat* and *λ* also had moderate influence on predicted soil water content. The predicted soil water content showed only slight to no-sensitivity to variations in all other parameters including variations in Kc and LAI at all sites. This implies that vegetation might not be a major driver of spatial variations in soil water. This could be due to the fact that water uptake by plants is quickly replaced by the upward flux from the shallow water table (Barquin *et al.*, 2011).

Again due to brevity only Sobol' analysis results for site 4 are presented, as results from the other sites were similar (Figure 3). Sobol' analysis confirmed Morris screening results indicating that saturated soil water content was the most important parameter explaining variations in predicted soil water content as measured by NSE and RMSE (as goodness-of-fit statistics were used as a summary measure of model output) at all sites. The fraction of the total variation in predicted soil and limestone bedrock water content explained by variation in each of the ten important parameters is represented using first order and total order Sobol sensitivity indices along the vertical axis (Figure 3). The first bar represents first order effects, while the second represents total order effects (quantifies the overall effect of a factor on model output) and the difference between the two bars represents parameter interactions.

Results also show that soil water dynamics are influenced by the parameters differently in the soil and limestone bedrock layers. In the soil layer (top 20 cm), unsaturated flow was mainly governed by θ_s, θ_r, α and n and the effects of parameter interactions were greater than in the limestone bedrock layer. In the limestone bedrock layer, unsaturated flow was mainly governed by θ_s and the first order effects approached 100% indicating that WAVE behaved as an additive model within the limestone bedrock layer particularly at sites 3 and 4 where sensors at 30 and 40 cm were close to saturation for the majority of the study. This is probably due to the fact that the differential capacitance term of Richards' equation (Equation 1) approaches zero under saturated conditions (Vanclooster *et al*. 1995). WAVE behaving as an additive model at 30 and 40 cm depth indicated that it could be calibrated using accurately measured soil and limestone bedrock water content data with less uncertainty in estimated parameter values. The results from sensitivity analysis indicate that future investigations of soil water dynamics within the C-111 basin should focus resources on proper characterization of soil hydraulic properties in order to develop models that can be used to explore soil water response to regional water management and possibly climate variability with less uncertainty.

Estimated parameters after calibration show that the average values of hydraulic parameters were not substantially different among calibrated values at each site (Table 5) implying that if the goal is not to simulate exact values of soil water but rather general trends in soil water content responses to different driving factors, average values of estimated parameters can be used anywhere within the study area. Estimated θ_s were compared to saturated soil and limestone bedrock water content when the sensors were below the water table and the values were in close agreement. For example, at site 3 θ_s (when the sensor were below water table) was identified as 35 (m^3/m^3) and the manually estimated values for layers 1 and 2 were 35 and 34, respectively. It has been shown by Evett et al. (2012) that under wet conditions there tends to be less spatial variability in soil water content and that EnviroScan data are more accurate under these conditions. We attributed difficulty of achieving a perfect fit between measured and predicted soil water content at various depth at the same site and across the different four sites to the following factors: 1) uncertainty in measured data, 2) intrinsic spatial variability in soil and limestone hydraulic parameters, and 3) exclusion of irrigation water applied from the conceptual model.

Soil water content prediction

Comparison between simulated and measured volumetric water content from capacitance probes at 10, 20, 30, and 40 cm depths under current canal stage operation criteria along C-111 were plotted (Figs. 5 to 8). Visual inspection indicates that WAVE was able to reproduce temporal variations in soil water content as influenced by seasonal variations in rainfall, evapotranspiration, and canal stage (Fig. 4). Some substantial deviations between predicted and measured volumetric water content at some sites and monitoring depths were observed particularly during the summer of 2011 months (May to October) which also corresponded to the lowest recorded soil water content.

Although the model was able to show the wetting and drying cycles during the summer of 2011(Figs. 5 to 8), these cycles substantially deviated from the measured trends probably due to the fact that the hydraulic parameters of the soil water retention curve that were estimated in the laboratory and whose ranges were used in the calibration may not have been representative of the spatially variable soil properties in field. This highlights the need for in-situ determination of soil water retention curves. The apparent contradiction in soil water content trends during the months June and July of 2011 in which the model indicated continued wetting conditions while the measured soil water indicated drying conditions could be attributed to the unexplained drop in potential evapotranspiration during this time period as shown in (Fig. 4). We speculate that meteorological data for the months of June and July 2011obtained from the Florida Automated Weather Network Station located approximately 10 km away from the study site, which was used in this study, might not have been accurate. Alternatively the long distance between the ET station and the study site could also have been a factor or errors in gauge adjusted NEXRAD rainfall data.   Small scale heterogeneity in soil properties amplified under dry conditions cause the geometric constant of the sensor to change with each measurement depth and access tube, which results in a different resonant frequency and variable water content estimates even if mean water content around the access tube is the same (Evett *et al.*, 2012). The increase in small scale variability in soil water content under dry conditions is compounded by the small volumes sensed by capacitance sensors. For example, EnviroScans measure an effective distance of only 3-5 cm from the access tube and may be affected by non-isothermal conditions and soil bulk electrical conductivity (Evett *et al.*, 2009).

Missing data at 10 cm depth and large deviation between predicted and measured soil water content at site 2 (Figure 5) during the first months of the study was due to poor sensor installation which was subsequently re-installed thus improving data at 20, 30 and 40 cm but re-installation did not improve data 10 cm at this site. It is worth noting that transformation of measured data using the capacitance sensor calibration equation developed in the laboratory by

Al-Yahyai *et al*. (2006) for gravely loam soils of south Florida was tried but gave inconsistent results at various depths and sites and was abandoned.

Goodness-of-fit statistics for model validation for the different sites and monitoring depth without and with consideration of measurement uncertainty were calculated (Tables 6 and 7). Fit between measured water content and simulated water content were unsatisfactory for all sites and the model was rejected (Ritter and Munoz, 2013) at all sites and depths with the exception of 30 and 40 cm depths at site 1 when uncertainty in measured soil water content was not taken into account (Table 6). This outcome is expected when performance is evaluated using measured data with high uncertainty without consideration of uncertainty boundaries in estimating the deviation between measured and predicted values. However, when uncertainty in measured soil water content data was considered by assuming a uniform probability distribution and using the procedure proposed by Harmel et al. (2010), there was an improvement in the Goodness-of-fit measures (Table 7) sometime substantially. Goodness-of-fit calculated using this approach would be more appropriate for evaluating model performance compared to simply using measured values which are inherently uncertain, despite its weakness of assuming symmetry. Future research could explore developing statistical methodologies for modifying the deviation between measured and predicted value based on asymmetric probability distributions.

Goodness-of-fit were re-evaluated at all the sites and monitoring depth and results considering asymmetric error boundaries and results presented in Table 8. There was more substantial improvements in Goodness-of-fit statistics especially at sites were the measured soil water overestimated simulated soil water. Model performance under the PER approach was acceptable at 11 out of the 16 monitoring depth compared to 7 out of 16 monitoring sites based on probability distribution approach which is more strict in terms of error modification (Harmel et al. 2010). The enhanced goodness-of-fit using the PER approach could be attributed to the fact that this method minimizes the calculated deviation between predicted and observed and thus produces minimum estimate of the error. Similar results were obtained by Harmel and Smith (2007) when evaluating water quality models.

Evaluation of Soil Water Response to Proposed Incremental Raises in Canal Stage

Soil water responses to proposed changes in canal stage management are shown in Figures 9 to 11. At site 2, after the proposed raises in canal C-111 stage, model predictions indicated no substantial differences in soil water content both during the wet and dry seasons. In the top 20 cm soil layer, soil water content did not reach saturation even after the maximum proposed increment in canal stage of 12 cm. This implies that farmlands with ground surface elevation similar to that at site 2 i.e., greater than 2.0 m NGVD29 are predicted to not experience root zone saturation after the proposed incremental raises in canal stage.

At site 3, changes in canal stage did result in observable changes in soil water content both during the wet season and dry season (Figure 10). Saturation was not reached within the top 10 cm but water content reached saturation at 20 cm depth after increasing canal stage by more than 9 cm and this condition persisted till late January of 2012 (Figure 10). This implies that growing periods for crop production would be greatly reduced. Although saturation at 30 and 40 cm (Figure 10) is not expected to hinder aeration in the root zone since the roots of the crops grown in this area never penetrate the limestone bedrock, it might exacerbate the problem of temporary groundwater flooding due to the phenomenon of groundwater ridging. These results predict that farmlands with land surface elevation similar to that of site 3 (1.19 m NGVD29) might be impacted by increases in canal stage greater than 9 cm.

The response at site 4 was similar to that observed at site 3 probably due to similar elevation (1.2 m NGVD29) (Figure 11). However, saturated conditions were not predicted for the top 10 cm during the growing season for increases in canal stage less than 9 cm but soil water content approached saturation during the wet season. The changes in canal stage resulted in saturated conditions at 30 and 40 cm during both in wet and dry seasons (Figure 11). Based on the period (January 2012 to February 2013) investigated for potential impacts of raising canal stage on root zone soil water content, the sites with land surface elevation greater than 2.0 m NGVD29 did not experience saturated conditions in the top 20 cm soil layer. Raising canal stage by more than 9 cm is predicted (within uncertainty ranges in Tables 7 and 8) to result in saturated root zone and shortening of the growing season at sites with land surface elevation less than 2.0 m NGVD29, which is critical for continued use of the land for agricultural production.

Application of this model is limited to exploratory assessments due to the uncertainty in measured data. This uncertainty could be reduced by improving the method for obtaining soil water content data that is used in model calibration. This is a very challenging proposition for this particular study site due to the complex texture of the soil, being composed of limestone bedrock that has been rock plowed. Soil water equipment that senses a larger soil volume and are not impacted by soil texture effects, temperature and salinity should be explored for measuring soil water content at this site. Future investigations with these models would also benefit from high resolution digital elevation maps that could be linked to the vadose zone model to identify areas with potential to experience transient root zone saturation.

Conclusion

Soil water dynamics in response to surface water management in the C-111 basin of Florida were simulated considering measurement uncertainty. Parameter screening using Morris method indicated that predicated soil water content was most sensitive to parameters of the van Genuchten equation. Quantitative variance based sensitivity analysis using Sobo's identified saturated soil water content as the most important input factor. The model behavior was nonadditive in the top 20 cm with various parameter interactions, and approximated an additive model in the usually saturated limestone layer.

Model performance was unsatisfactory without consideration of measurement uncertainty. However, NSE increased and RMSE decreased when uncertainty in measured data were considered during model performance evaluation. Accounting for uncertainty using probability error ranges resulted in more substantial improvements in goodness-of-fit compared to accounting for uncertainty using measurement probability distributions. As demonstrated in this study it is more appropriate to calculate deviations between measured and predicted values based on uncertainty boundaries or probability distributions of measured data than simply using a single measured value which are inherently uncertain. However, we caution that poor model performance due to inaccurate model structure, errors in boundary conditions or input data should not be judged as good model performance simply because of integrating of uncertainty in model evaluation but rather models should be judged on their ability to represent the physical processes. This suggests that parameterizing the model using the measured soil water content without consideration of measurement uncertainty would likely result in a model calibrated to the collected data rather than to the system or over calibration.

Model application to predict soil water dynamics under raised canal stage indicated that sites with land surface elevation of less than 2.0 m NGVD29 might experience transient root zone saturation and shortening of the growing season if canal stage is raised more than 9 cm. At depths greater than 20 cm, raises in canal stage were predicted to result in prolonged saturated conditions. The saturated conditions at the 30 and 40 cm depth at low elevation sites could exacerbate the problem of temporary groundwater flooding due to groundwater ridging suggesting that water management practices would need to be modified.

The models developed in this study could be could be combined with high resolution digital elevation models (DEM) in future studies to identify areas that should not be planted to minimize potential losses. The study also highlighted the need to develop methodologies for modifications of the error term between predicted and observed based on asymmetric measurement probability distributions.

Acknowledgements

We would like to thank the anonymous reviewers for the useful suggestions that helped improve the quality of the manuscript. The authors would also like to thank the South Florida Water Management District for providing the funding for this study, Mr. Vito Strano and Mr. Sam Accursio for allowing us to use their lands and Ms. Tina Dispenza for her contribution towards data collection and processing.

References

Al-Yahyai R, Schaffer B, Davies FS, Muñoz-Carpena R. 2006. Characterization of Soil-Water Retention of a Very Gravelly-Loam Soil Varied with Determination Method. *Soil Science.* 171(2): 85–93. DOI:10.1097/01.ss.0000187372.53896.9d.

Barquin LP, Migliaccio KW, Muñoz-Carpena R, Schaffer B, Crane JH, Li YC. 2011. Shallow Water Table Contribution to Soil-Water Retention in Capillary Fringe of a Very Gravelly Loam Soil of South Florida. *Vadose Zone J*, 10:1–8.

Bilskie J. 2001. Soil water measurements: Considering variability and uncertainty. App. Note: 2S J. Campbell Scientific, Logan Utah.

Chen M, Willgoose GR, Saco PM. 2012. Spatial prediction of temporal soil moisture dynamics using HYDRUS-1D. *Hydrological Processes*. DOI: 10.1002/hyp.9518

Evett SR, Schwartz RC, Casanova JJ, Heng LK. 2012. Soil water sensing for water balance, ET and WUE. *J. Agricultural Water Management.* 104:1–9.

Evett SR, Schwartz RC, Tolk JA, Howell TA. 2009. Soil profile water content determination: spatio-temporal variability of electromagnetic and neutron probe sensors in access tubes. *Vadose Zone J*. 8 (4), 1–16.

Evett SR. 2000. Some Aspects of Time Domain Reflectometry (Tdr), Neutron Scattering, and Capacitance Methods of Soil Water Content Measurement. Pp. 5-49 In Comparison of soil water measurement using the neutron scattering, time domain reflectometry and capacitance methods. International Atomic Energy Agency, Vienna, Austria, IAEA-TECDOC-1137.

Feddes RA, Kowalik PJ, Zaradny H. 1978. Simulation of field water use and crop yield. Simulation Monographs. PUDOC, Wageningen, The Netherlands.

Gabriel JL, Lizaso JI, Miguel Q. 2010. Laboratory versus Field Calibration of Capacitance Probes. *Soil Sci Soc Am* J. 74:593-601.

Germann P, Levy B. 1986. Groundwater response to precipitation. *EOS*, 67: 91.

Harmel RD, Smith PK, Migliaccio K. 2010. Modifying goodness-of-fit indicators to incorporate both measurement and model uncertainty in model calibration and validation. *Trans. ASABE* 53(1): 55-63.

Harmel RD, Smith PK. 2007. Consideration of measurement uncertainty in the evaluation of goodness-of-fit in hydrologic and water quality modeling. J. Hydrology. 337: 326–336.

IAEA. 2008. Field Estimation of soil water content; A practical guide to methods, instrumentation and sensor technology. Training Course Series No. 30, International Atomic Energy Agency, Vienna, Austria.

Kavetski D, Kuczera G, Franks SW. 2006. Bayesian analysis of input uncertainty in hydrological modeling, *Water Resour. Res*., 42, W03408, doi:10.1029/2005WR004376.

Kayane I, Kaihotsu I. 1988. Some Experimental Results Concerning Rapid Water Table Response to Surface Phenomena. *J. Hydrology*, 102: 215-234.

Kisekka I, Migliaccio KW, Muñoz-Carpena R, Khare Y, Boyer TH. 2013a. Sensitivity analysis and parameter estimation for an approximate analytical model of canal-aquifer interaction applied in the C-111 Basin. In-press *Trans. ASABE* SW-10037-2012.

Kisekka I, Migliaccio KW, Muñoz-Carpena R, Li YC, Boyer. T. H. 2013b. Simulating Water Table Response to Proposed Changes in Surface Water Management in Agricultural Lands Adjacent to Everglades National Park. Under peer review *Journal of Agricultural Water Management*.

Kisekka I, Migliaccio KW, Muñoz-Carpena R, Schaffer B. 2013c. Dynamic Factor Analysis of Surface Water Management Impacts on Soil and Bedrock WaterContents in Southern Florida Lowlands. *Journal of Hydrology*. http://dx.doi.org/10.1016/j.jhydrol.2013.02.035

Lin C. 2003. Frequency Domain Versus Travel Time Analyses of TDR Waveforms for Soil Moisture Measurements. *Soil Science Society of America Journal* 67(3):720-729.

Lizaso JI, Ritchie JT. 1997. Maize Shoot and Root Response to Root Zone Saturation during Vegetative Growth. *Agron. J*. 89:125-134.

Mualem Y. 1976. A new model for predicting the hydraulic conductivity of unsaturated porous media. *Water Resour. Res*. 12, 513–522.

Muñoz-Carpena R, Ritter A, Bosch DD, Schaffer B, Potter TL. 2008. Summer cover crop impacts on soil percolation and nitrogen leaching from a winter corn field. *Agricultural Water Management* 95:633–644.

Muñoz-Carpena R, Zajac Z, Kuo Y. 2007. Global Sensitivity and uncertainty Analyses of the Water Quality Model VFSMOD-W. Trans. ASABE 50(5):1719-1732.

Politis, D.N., Romano, J.P., 1994. The stationary bootstrap. J. Amer. Statist. Assoc. 89, 1303–1313

Ritter A, Muñoz-CarpenaR. 2013. Predictive ability of hydrological models: objective assessment of goodness-of-fit with statistical significance. J. Hydrology. 480(1):33-45. doi:10.1016/j.jhydrol.2012.12.004

Ritchie JT. 1972. Model for predicting evaporation from a row crop with incomplete cover. Water Resources Research 8(5): 1204–1213. DOI:10.1029/WR008i005p01204

Saltelli A, Tarantola S, Campolongo F, Ratto M. 2004. Sensitivity Analysis in Practice: A Guide to Assessing Scientific Models. Chichester, U.K.: John Wiley and Sons.

Schaffer B.1998. Flooding Responses and Water-use Efficiency of Subtropical and Tropical Fruit Trees in an Environmentally-sensitive Wetland. *Annals of Botany* 81: 475–481.

Sentek Pty Ltd. 2001. Calibration of the Sentek Pty Ltd Soil Moisture Sensors. Stepney, South Australia. Soil Survey Division Staff. 1993. Soil survey manual.

USACE and SFWMD. 2011. Comprehensive Everglades Restoration Plan: C-111 spreader canal western project: Final Integrated Project Implementation Report and Environmental Impact Statement. U.S. Army Corps of Engineers Jacksonville, District.

van Genuchten MTh, Leij, FJ and Yates. SR. 1991. The RETC Code for Quantifying the Hydraulic Functions of Unsaturated Soils, Version 1.0. EPA Report 600/2-91/065, U.S Salinity Laboratory, USDA-ARS, Riverside, California.

van Genuchten MT. 1980. A closed-form equation for predicting the hydraulic conductivity of soil. *Soil Sci. Soc. Am. J*. 44:892–898.

Vanclooster M, Viaene P, Diels J, Christiaens K. 1996. WAVE: A mathematical model for simulating water and agrochemicals inthe soil and vadose environment. Reference and user's manual (release2.0). Institute for Land and Water Management, Katholieke Universiteit Leuven, Leuven, Belgium.

Vanclooster M, Viaene P, Diels J, Feyen J. 1995. A deterministic evaluation analysis applied to an integrated soil-crop model. *Ecological Modelling*. 81:183-195.

Waswa GW, Clulow C. FreeseLe Roux PAL, Lorentz SA. 2013. Transient Pressure Waves in the Vadose Zone and the Rapid Water Table Response. *Soil Sci Soc Am* J. doi:10.2136/vzj2012.0054.

Table 1. WAVE calibration and validation periods at the different monitoring sites for soil water content

Sites	Calibration	Validation
1	04/21/2011 to 12/31/2011	01/01/2012 to 02/28/2013
2	01/21/2011 to 12/31/2011	01/01/2012 to 02/28/2013
3	10/01/2010 to 09/30/2011	10/01/2011 to 02/28/2013
4	01/26/2011 to 12/31/2011	01/01/2012 to 02/28/2013

Table 2. Parameters used in WAVE for simulating soil water content at four sites within the C-111 basin assuming a uniform distribution for all parameters

Description	Parameter	Value	Source
Layer 1			
Saturated soil water content ($m^3\ m^{-3}$)	θ_{s1}	0.20-0.46	Measured[d]
Residual soil water content ($m^3\ m^{-3}$)	θ_{r1}	0.0-0.092	Measured
Inverse of the air entry value (cm^{-3})	α_1	0.003-0.093	Measured
Curve shape parameter	n_1	1.0-1.2	Measured
Pore connectivity parameter[a]	λ_1	0.10-1.10	Literature
Unsaturated hydraulic conductivity (cm/day) [b]	K_1	500-1551	Literature
Maximum water uptake rate (day^{-1})[c]	$Smax1$	0.01-0.014	Literature
Layer 2			
Saturated soil water content ($m^3\ m^{-3}$)[d]	θ_{s2}	0.20-0.46	Literature
Residual soil water content ($m^3\ m^{-3}$)[b]	θ_{r2}	0.0-0.01	Literature
Inverse of the air entry value (cm^{-3})[b]	α_2	0.009-0.15	Literature
Curve shape parameter[b]	n_2	0.9-1.2	Literature
Pore connectivity parameter[a]	λ_2	0.10-4.5	Literature
Unsaturated hydraulic conductivity (cm/day)[b]	K_2	5000-14000	Literature

[a]Obtained from Mualem (1976)
[b]Obtained from Muñoz-Carpena *et al.* (2008)
[c]Obtained from Vanclooster *et al*. (1995)
[d]Estimated from measured data

Table 3. Crop coefficient (Kc) and leaf area index (LAI) values used in a discrete uniform distribution in the sensitivity analysis of simulated soil water content

Development stage	Kc[a] value	Kc symbol	LAI[b]	LAI symbol
Initial	0.6	Kc1	0.5	LAI1
Mid-season	1.1	Kc2	2.9	LAI2

Late-season	0.85	Kc3	1.45	LAI3

[a]Crop coefficient, value obtained from Muñoz-Carpena et al. (2008)
[b]Leaf area index, value measured

Table 4. Morris screening results for WAVE model applied at site 4

Soil depth	10 cm		20 cm		30 cm		40 cm	
Parameter	μ*[c]	σ [d]	μ*	σ	μ*	Σ	μ*	σ
Residual water content[a] (m^3/m^3)	4.3	5.7	2.4	2.9	0.0	0.0	0.0	0.0
Residual water content[b] (m^3/m^3)	0.0	0.0	0.3	0.4	1.4	1.4	2.0	2.0
Saturated water content[a] (m^3/m^3)	24.2	16.7	16.0	14.7	0.1	0.1	0.0	0.1
Saturated water content[b] (m^3/m^3)	0.0	0.1	11.8	11.4	69.4	49.9	120.1	105.3
Inverse of air entry value[a] (cm^{-1})	7.7	6.9	4.5	5.1	0.3	0.3	0.2	0.3
Inverse of air entry value[b] (cm^{-1})	2.1	2.8	8.9	7.6	33.6	27.7	50.4	43.6
Curve shape parameter[a]	14.3	10.8	9.1	6.7	0.2	0.4	0.2	0.3
Curve shape parameter[b]	0.9	1.3	9.7	11.9	31.8	16.0	45.7	26.0
Saturated hydraulic[a] (m/d)	0.2	0.5	0.1	0.2	0.2	0.3	0.1	0.2
Saturated hydraulic conductivity[b] (m/d)	1.1	2.5	1.3	2.5	0.7	0.8	0.5	0.7
Pore connectivity parameter[a]	0.1	0.3	0.1	0.3	0.1	0.1	0.1	0.1
Pore connectivity parameter[b]	0.7	1.1	1.0	1.5	1.0	1.4	0.9	1.1
Crop coefficient initial stage	0.0	0.0	0.0	0.0	0.0	0.0	0.0	0.0
Crop coefficient mid-season stage	0.0	0.0	0.0	0.0	0.0	0.0	0.0	0.0
Crop coefficient late-season stage	0.4	0.7	0.2	0.4	0.1	0.2	0.1	0.1
Leaf area index initial stage	0.0	0.0	0.0	0.0	0.0	0.0	0.0	0.0
Leaf area index mid-season stage	0.0	0.0	0.0	0.0	0.0	0.0	0.0	0.0
Leaf area index late-season stage	0.1	0.2	0.0	0.1	0.0	0.0	0.0	0.0
Maximum root water uptake	0.0	0.0	0.0	0.0	0.0	0.0	0.0	0.0

[a]Layer 1 parameter (top 20 cm of soil profile)
[b]Layer 2 parameter (bottom 20 cm of soil profile)
[c]Absolute values of Morris sensitivity measure which assesses the overall effect of the factor
[d]Morris sensitivity measure which indicates effects of a factor's interactions with other factors

Table 5. WAVE parameters obtained from calibration at different sites (October 1, 2010 to December 31, 2011)

Parameter	Site 1	Site 2	Site 3	Site 4	Avg.
Layer 1 (top 20 cm)					
Residual water content (θ_r)	0.09	0.08	0.10	0.10	0.09
Saturated water content (θ_s)	0.30	0.32	0.34	0.30	0.31
Curve shape parameter (n)	1.09	1.22	1.17	1.15	1.14
Inverse of air entry value (α)	0.04	0.06	0.09	0.09	0.08
Pore connectivity parameter (λ)	0.50	0.62	0.54	0.62	0.58
Layer 2 (bottom 40 cm)					
Residual water content (θ_r)	0.09	0.06	0.09	0.09	0.08

Saturated water content (θ_s)	0.31	0.31	0.35	0.30	0.32
Curve shape parameter (n)	1.12	1.11	1.11	1.10	1.11
Inverse of air entry value (α)	0.08	0.10	0.10	0.09	0.10
Pore connectivity parameter (λ)	0.50	0.62	0.54	0.62	0.58
Sat. hydraulic conductivity (K)	8000	9307	8511	8419	8514

Table 6. Goodness-of-fit statistics without consideration of measurement uncertainty for WAVE water content simulations by soil depth during the validation period ranging from [01/01/2012 to 02/28/2013] at site 1 and [01/01/2012 to 02/28/2013] at other sites

		Site 1		
Depth	10 cm	20 cm	30 cm	40 cm
NSE[1]	0.26(-0.32-0.66)	0.35(0.03-0.59)	0.80(0.66-0.88)	0.77(0.74-0.88)
RMSE[2]	0.95(0.72-1.19)	0.62(0.52-0.73)	0.35(0.31-0.41)	0.48(0.41-0.54)
A[3] (%)	0.0	0.0	0.5	0.5
B[4] (%)	0.0	0.0	51.4	29.1
C[5] (%)	3.1	0.5	46.4	54.3
D[6] (%)	93.9	99.5	1.7 (**)	16.1
		Site 2		
NSE	-2.79(-6.21—1.3)	0.57(0.28-0.76)	0.44(0.27-0.57)	0.10(-0.90-066)
RMSE	1.16(0.94-1.37)	0.81(0.71-0.96)	0.84(0.65-1.06)	1.35(0.94-1.72)
A (%)	0.0	0.0	0.0	0.0
B (%)	0.0	0.6	0.0	0.0
C (%)	0.0	67.1	0.1	0.0
D (%)	100.0	32.3	99.1	100.0
		Site 3		
NSE	0.25(-0.24-0.50)	0.30(-0.66-0.60)	-1.95(-5.5--0.17)	-3.80(-6.2--0.87)
RMSE	1.42(1.16-1.66)	0.63(0.52-0.81)	0.99(0.73-1.22)	0.89(0.55-1.28)
A (%)	0.0	0.0	0.0	3.2
B (%)	0.0	0.0	0.0	5.3
C (%)	0.0	2.6	0.0	10.4
D (%)	100.0	97.4	100.0	81.1
		Site 4		
NSE	-0.35(-1.80-0.45)	0.31(-0.99-0.66)	-0.63(-2.11-0.01)	-12.2(-29.6--4.18)
RMSE	0.95(0.63-1.29)	0.52(0.41-0.66)	0.63(0.43-0.80)	0.97(0.79-1.11)
A (%)	0.0	0.0	0.0	0.0
B (%)	0.0	0.1	0.0	0.0
C (%)	0.2	5.2	0.0	0.5
D (%)	99.8	94.7	100.0	99.5

[1]Nash-Sutcliffe coefficient (95% confidence interval)

[2]Root mean square error (95% confidence interval)

[3]A probability of fit being very good 0.9<NSE<1.0
[4]B probability of fit being good 0.8<NSE<0.9
[5]C probability of fit being acceptable 0.65<NSE<0.8
[6]D p-value, p-value < α => model acceptable while p-value > α => model rejected, α could be (***)1%, (**)5% or (*)10%

Table 7. Goodness-of-fit statistics considering measurement uncertainty for WAVE water content simulations by soil depth during the validation period ranging from [01/01/2012 to 02/28/2013] at site 1 and [01/01/2012 to 02/28/2013] at other sites

		Site 1		
Depth	10 cm	20 cm	30 cm	40 cm
NSE[1]	0.78(0.50-0.92)	0.87(0.75-0.93)	0.89(0.75-0.94)	0.85(0.68-0.93)
RMSE[2]	0.53(0.33-0.74)	0.28(0.20-0.39)	0.26(0.20-0.40)	0.38(0.31-0.51)
A[3] (%)	7.2	23.4	47.3	15.0
B[4] (%)	31.3	70.2	51.0	58.4
C[5] (%)	42.6	5.9	1.7	26.1
D[6] (%)	18.9	0.0 (***)	0.0 (***)	0.5 (***)
		Site 2		
NSE	-1.66(-5.39--0.3)	0.89(0.78-0.94)	0.88(0.79-0.93)	0.65(0.24-0.91)
RMSE	0.70(0.70-1.30)	0.41(0.31-0.55)	0.38(0.25-0.54)	0.81(0.43-1.13)
A (%)	0.0	41.2	37.2	4.6
B (%)	0.0	56.2	61.1	13.6
C (%)	0.0	2.6	1.7	33.4
D (%)	100.0	0.0 (***)	0.0 (***)	48.4
		Site 3		
NSE	0.81(0.59-0.89)	0.76(0.02-0.94)	0.70(0.25-0.91)	0.30(-0.31-0.88)
RMSE	0.71(0.53-0.93)	0.37(0.20-0.60)	0.32(0.21-0.42)	0.34(0.13-0.55)
A (%)	3.3	20.5	3.4	3.2
B (%)	54.7	23.6	19.1	5.3
C (%)	37.7	28.6	37.9	10.4
D (%)	4.3 (**)	27.3	39.6	81.1
		Site 4		
NSE	0.78(0.49-0.93)	0.87(0.39-0.97)	0.75(0.52-0.87)	-0.20(-1.95-0.54)
RMSE	0.39(0.22-0.54)	0.22(0.13-0.37)	0.24(0.14-0.33)	0.30(0.23-0.35)
A (%)	8.5	40.9	1.9	0.0
B (%)	34.6	35.0	25.6	0.0
C (%)	43.8	17.1	59.7	0.5
D (%)	13.1	0.7 (***)	12.8	99.5

[1]Nash-Sutcliffe coefficient (95% confidence interval)
[2]Root mean square error (95% confidence interval)
[3]A probability of fit being very good 0.9<NSE<1.0

[4]B probability of fit being good 0.8<NSE<0.9
[5]C probability of fit being acceptable 0.65<NSE<0.8
[6]D p-value, p-value < α => model acceptable while p-value > α => model rejected, α could be (***)1%, (**)5% or (*)10%

Table 8. Goodness-of-fit statistics considering asymmetric measurement uncertainty error boundaries (-5% lower error bound and +2.5% upper error bound) for WAVE water content simulations by soil depth during the validation period ranging from [01/01/2012 to 02/28/2013] at site 1 and [01/01/2012 to 02/28/2013] at other sites

		Site 1		
Depth	10 cm	20 cm	30 cm	40 cm
NSE[1]	0.97(0.96-0.98)	0.92(0.85-0.97)	0.97 (0.96-1.00)	0.99 (0.98-1.00)
RMSE[2]	0.16 (0.11-0.22)	0.21(0.14-0.30)	0.10 (0.05-0.15)	0.06 (0.04-0.09)
A[3] (%)	100.0	79.9	100.0	100.0
B[4] (%)	0.0	20.1	0.0	0.0
C[5] (%)	0.0	0.0	0.0	0.0
D[6] (%)	0.0 (***)	0.0 (***)	0.0 (***)	0.0 (***)
		Site 2		
NSE	0.26 (0.85-0.56)	0.92 (0.87-0.95)	0.85 (0.77-0.92)	0.86 (0.67-0.96)
RMSE	2.94 (2.12-3.63)	0.34 (0.25-0.43)	0.43 (0.28-0.59)	0.50 (0.26-0.71)
A (%)	0.0	88.0	11.3	30.3
B (%)	0.0	12.0	80.5	48.4
C (%)	0.7	0.0	8.2	20.5
D (%)	99.3	0.0 (***)	0.0 (***)	0.8 (***)
		Site 3		
NSE	0.81 (0.53-0.92)	0.88 (0.51-0.98)	0.73(0.25-0.91)	0.32 (-0.31-0.89)
RMSE	0.71 (0.51-0.96)	0.26 (0.12-0.43)	0.16 (0.10-0.32)	0.34(0.13-0.55)
A (%)	9.5	45.1	5.7	3.2
B (%)	46.9	35.8	49.5	5.3
C (%)	36.2	16.6	35.9	10.4
D (%)	7.4 (*)	3.5 (*)	8.9 (*)	81.1
		Site 4		
NSE	0.63 (0.14-0.90)	0.95 (0.69-0.99)	0.98 (0.97-1.00)	-1.06 (-4.14-0.24)
RMSE	0.49 (0.25-0.70)	0.15(0.05-0.27)	0.10 (0.01-0.20)	0.39 (0.29-0.47)
A (%)	3.7	79.8	100.0	0.0
B (%)	12.1	16	0.0	0.0
C (%)	33.1	3.9	0.0	0.0
D (%)	51.1	0.3 (***)	0.0 (***)	100.0

[1]Nash-Sutcliffe coefficient (95% confidence interval)
[2]Root mean square error (95% confidence interval)
[3]A probability of fit being very good 0.9<NSE<1.0

[4]B probability of fit being good $0.8<NSE<0.9$
[5]C probability of fit being acceptable $0.65<NSE<0.8$
[6]D p-value, p-value $< \alpha \Rightarrow$ model acceptable while p-value $> \alpha \Rightarrow$ model rejected, α could be (***)1%, (**)5% or (*)10%

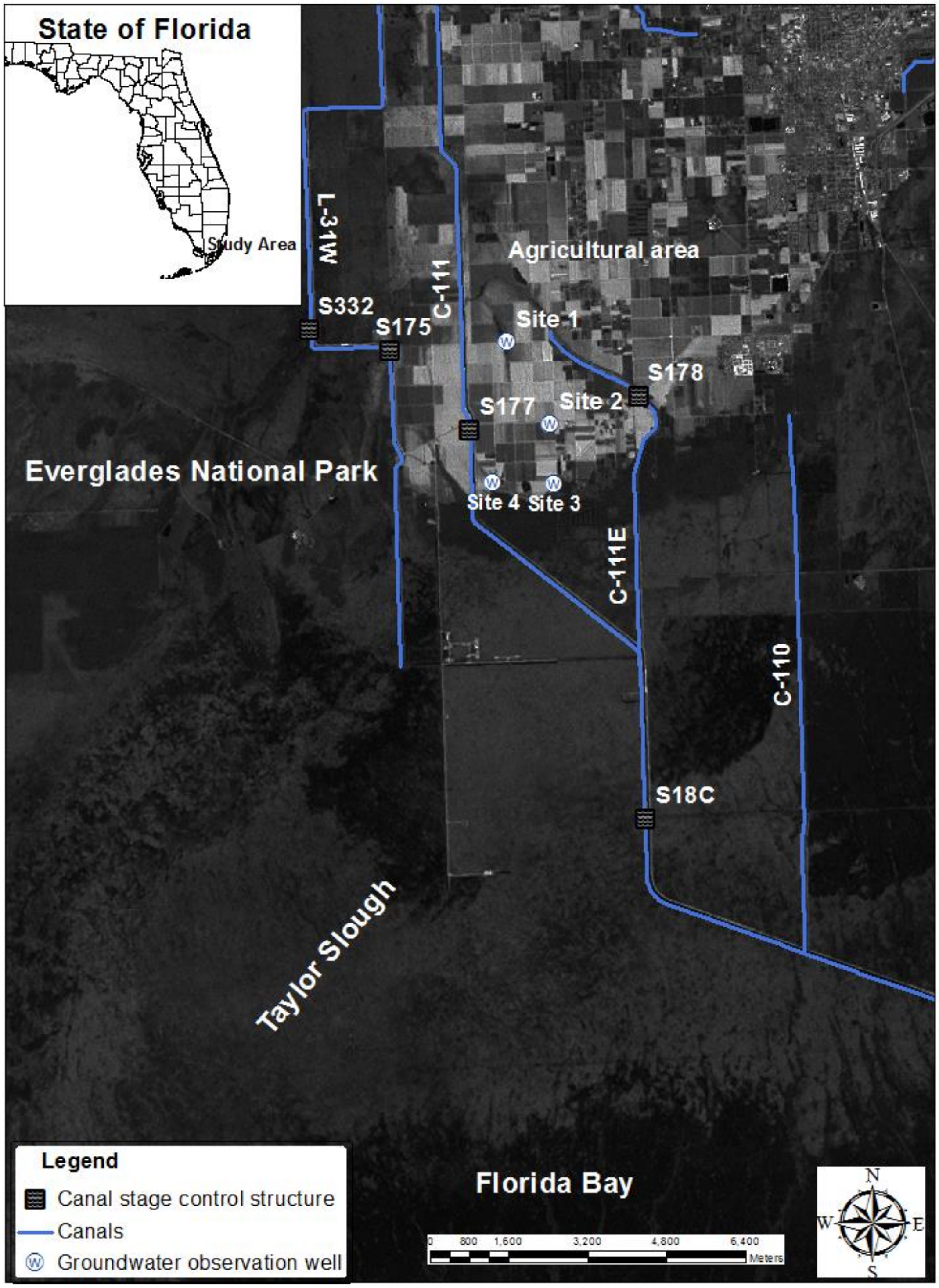

Figure 1. Showing soil water monitoring sites, agricultural lands adjacent to Everglades National Park, and canal network within the C-111 basin of south Miami-Dade County, Florida.

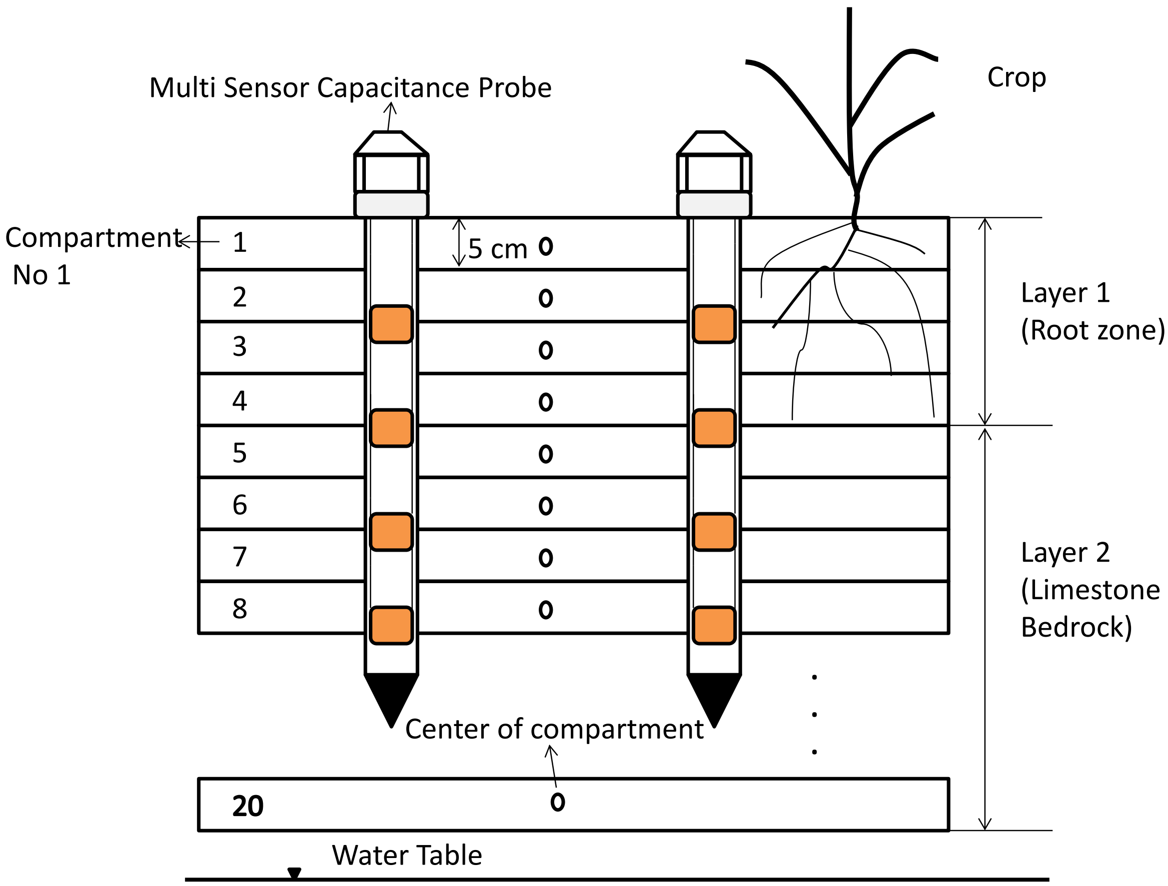

Figure 2. Depiction of the discretizing of the soil profile and location of the capacitance sensors

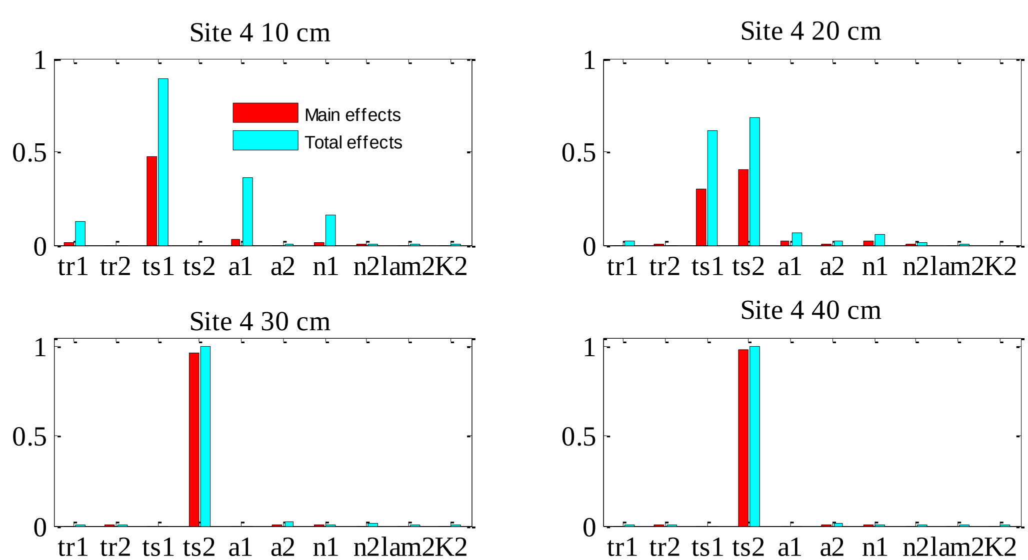

Figure 3. Sobol indices on the vertical axis and parameters (tr1 and tr2 are residual soil water content, ts1 and ts2 are saturated soil content, a1 and a2 are inverse of air entry value, n1 and n2 are curve shape parameter, lam is pore connectivity parameter, K2 is saturated hydraulic conductivity and 1 and 2 refer to the soil and limestone layers) for the WAVE model on the horizontal axis as applied to simulate volumetric soil water content at four monitoring depth 10, 20, 30 and 40 cm at site 4.

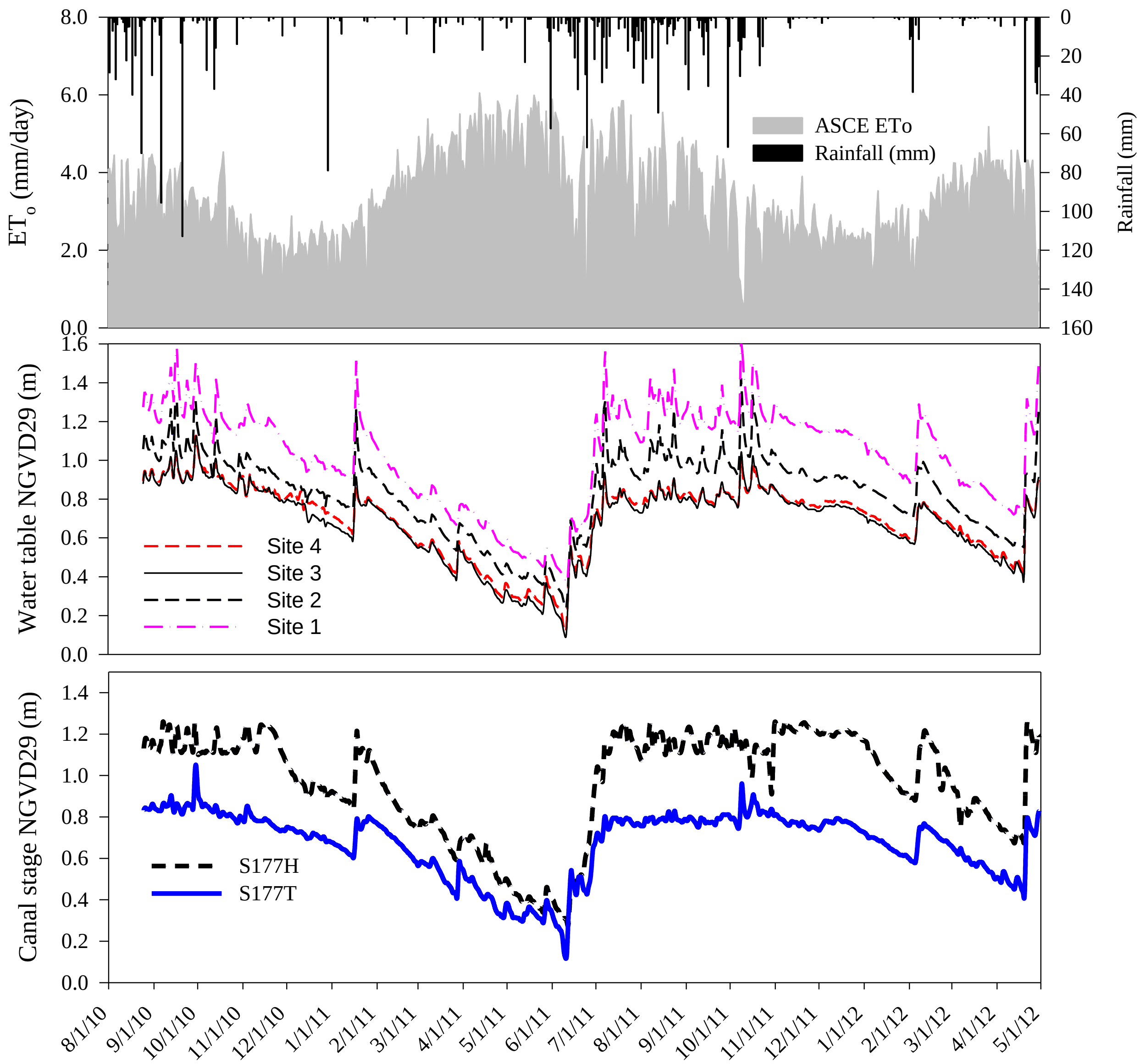

Figure 4. Showing model input variables evapotranspiration, rainfall and water table elevation as well as the canal stage which drives variations in water table elevation.

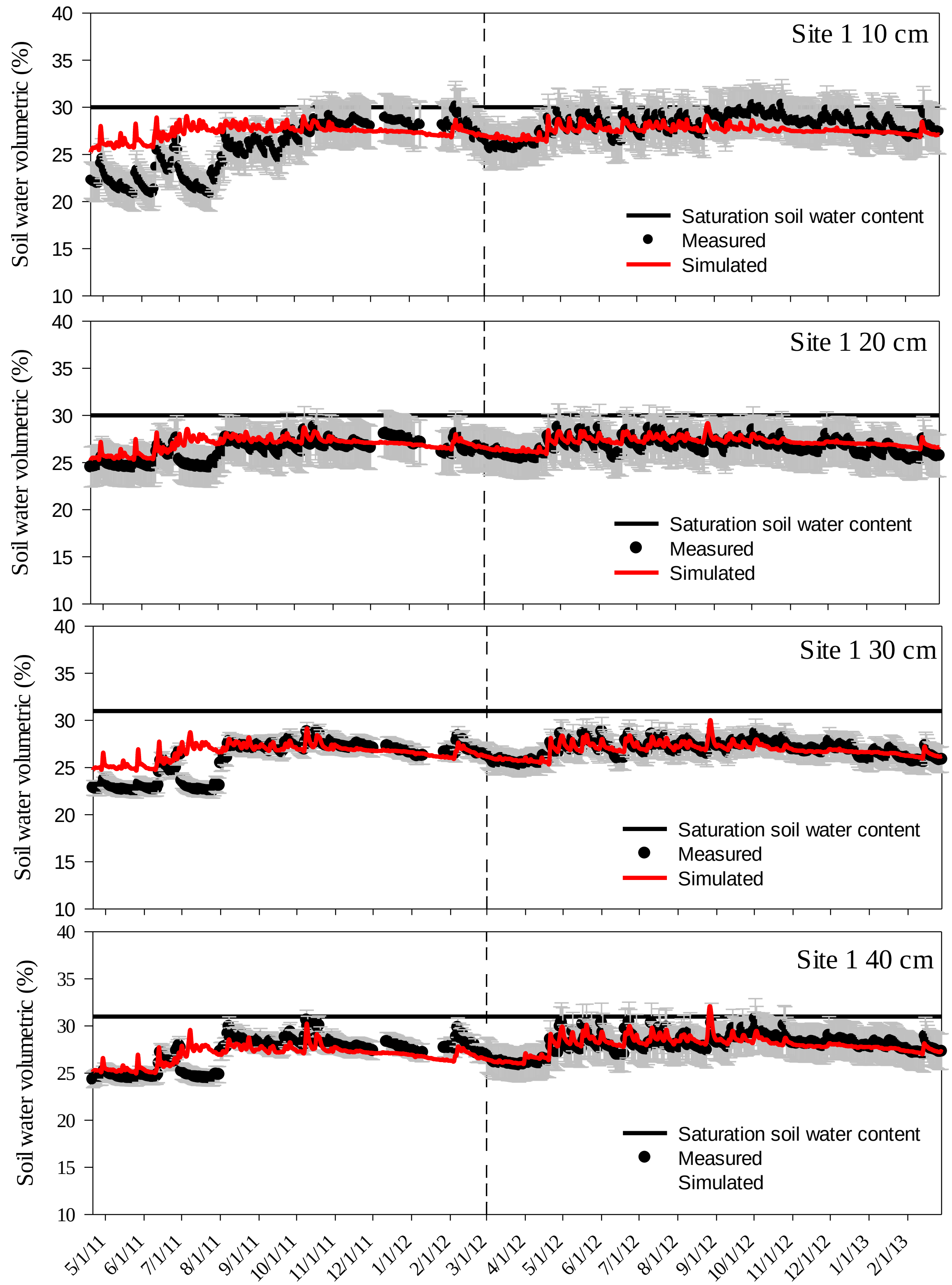

Figure 5. Comparison of WAVE simulated and measured volumetric soil water content (error bars indicate measurement uncertainty) at site 1 where the vertical line separates calibration and validation data sets.

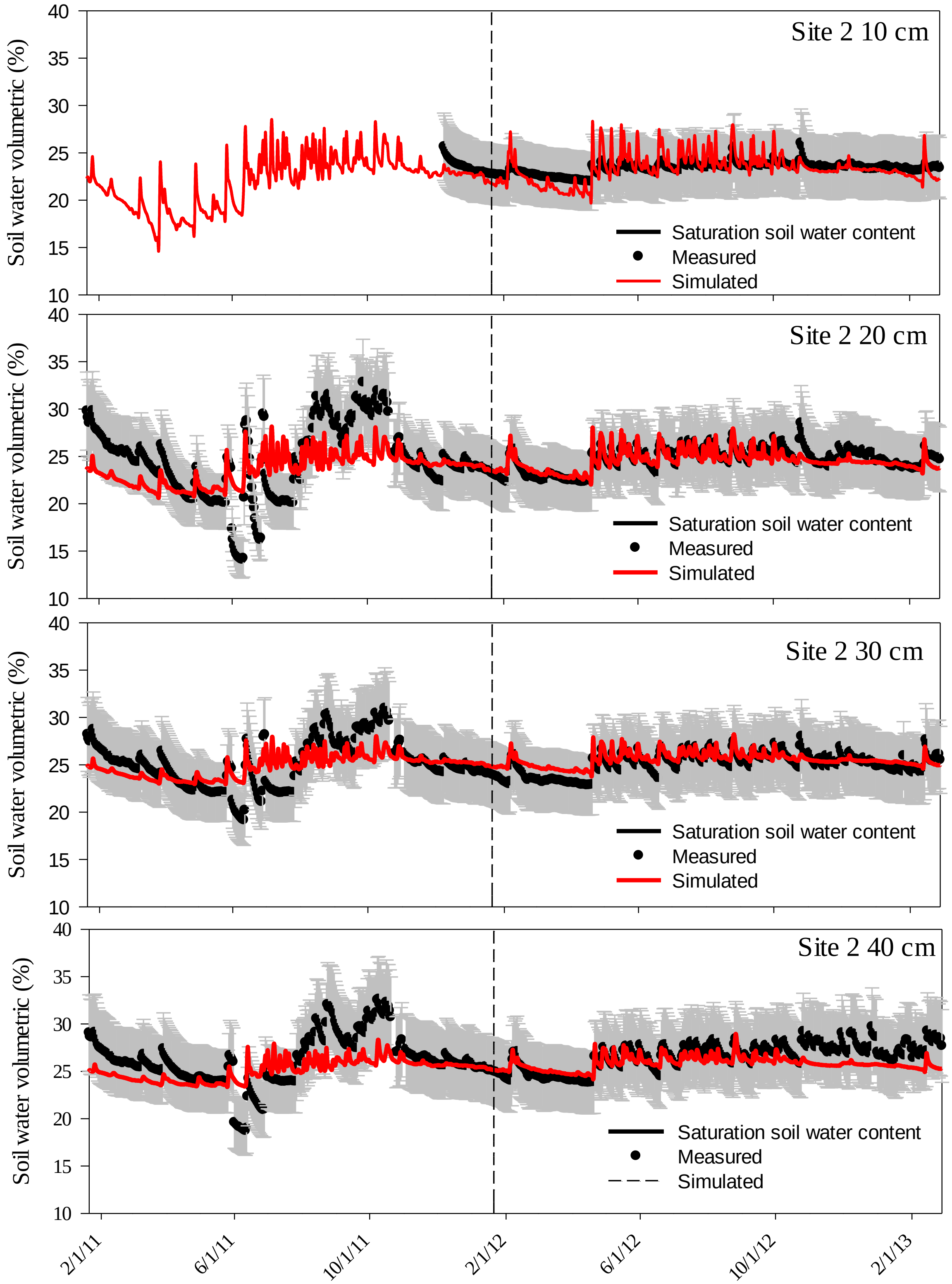

Figure 6. Comparison of WAVE simulated and measured volumetric soil water content (error bars indicate measurement uncertainty) at site 2 where the vertical line separates calibration and validation data sets.

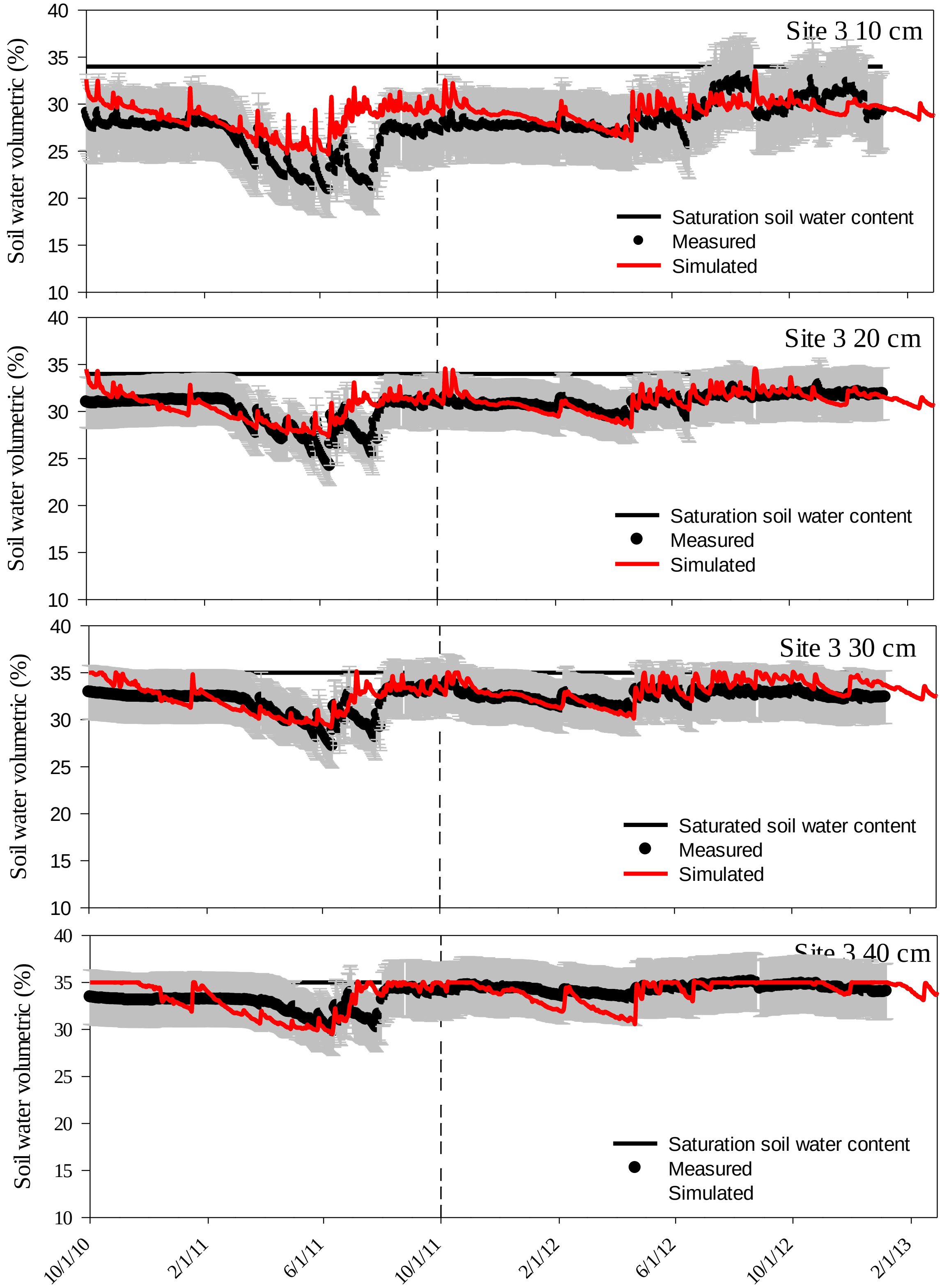

Figure 7. Comparison of WAVE simulated and measured volumetric soil water content (error bars indicate measurement uncertainty) at site 3 where the vertical line separates calibration and validation data sets.

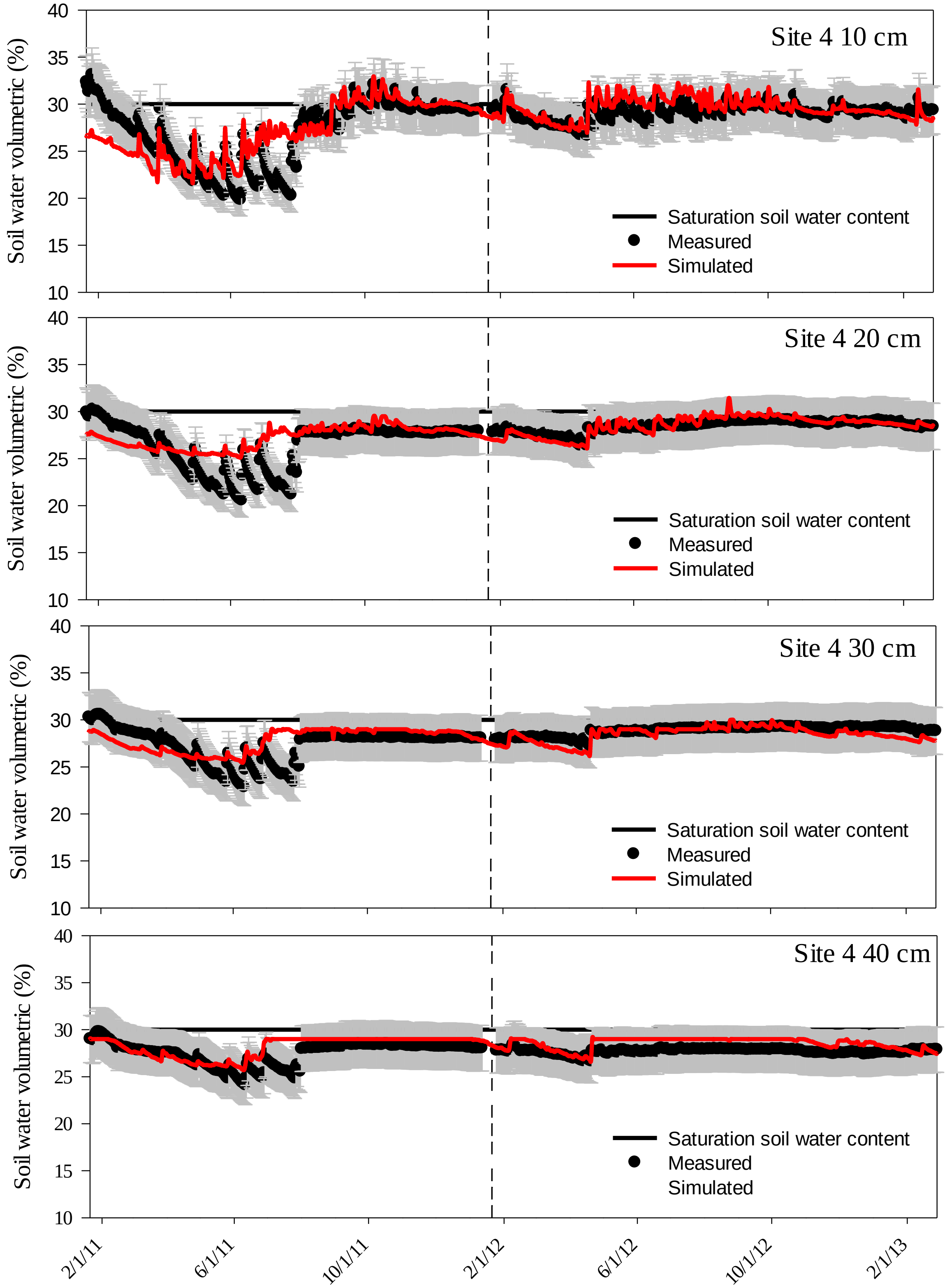

Figure 8. Comparison of WAVE simulated and measured volumetric soil water content (error bars indicate measurement uncertainty) at site 4 where the vertical line separates calibration and validation data sets.

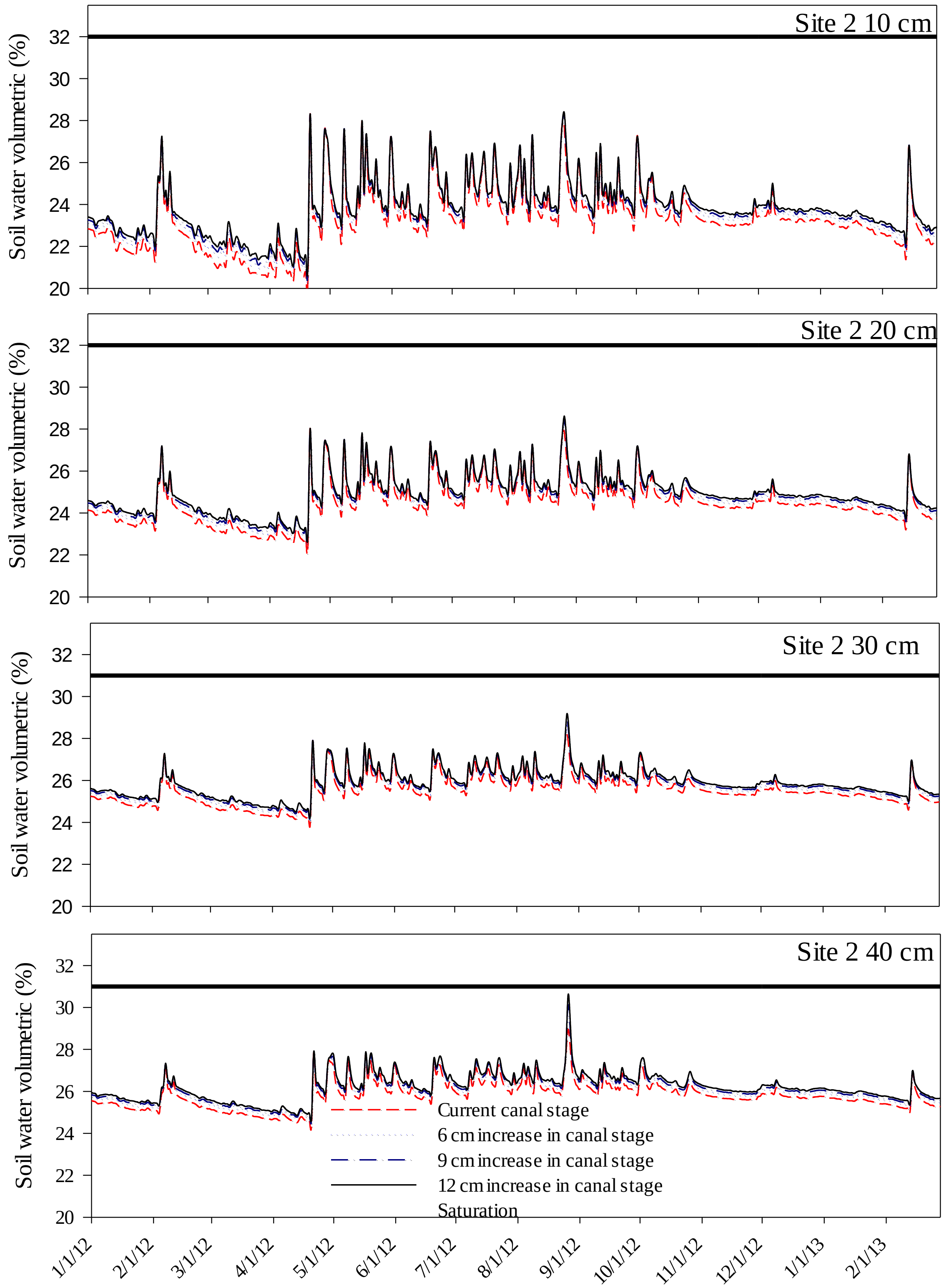

Figure 9. Simulated volumetric soil water content under different C-111 canal stage management scenarios at four different depth at site 2 [caution: absolute predictions should be regarded as qualitative assessments only due to uncertainty in measured data used in developing the model].

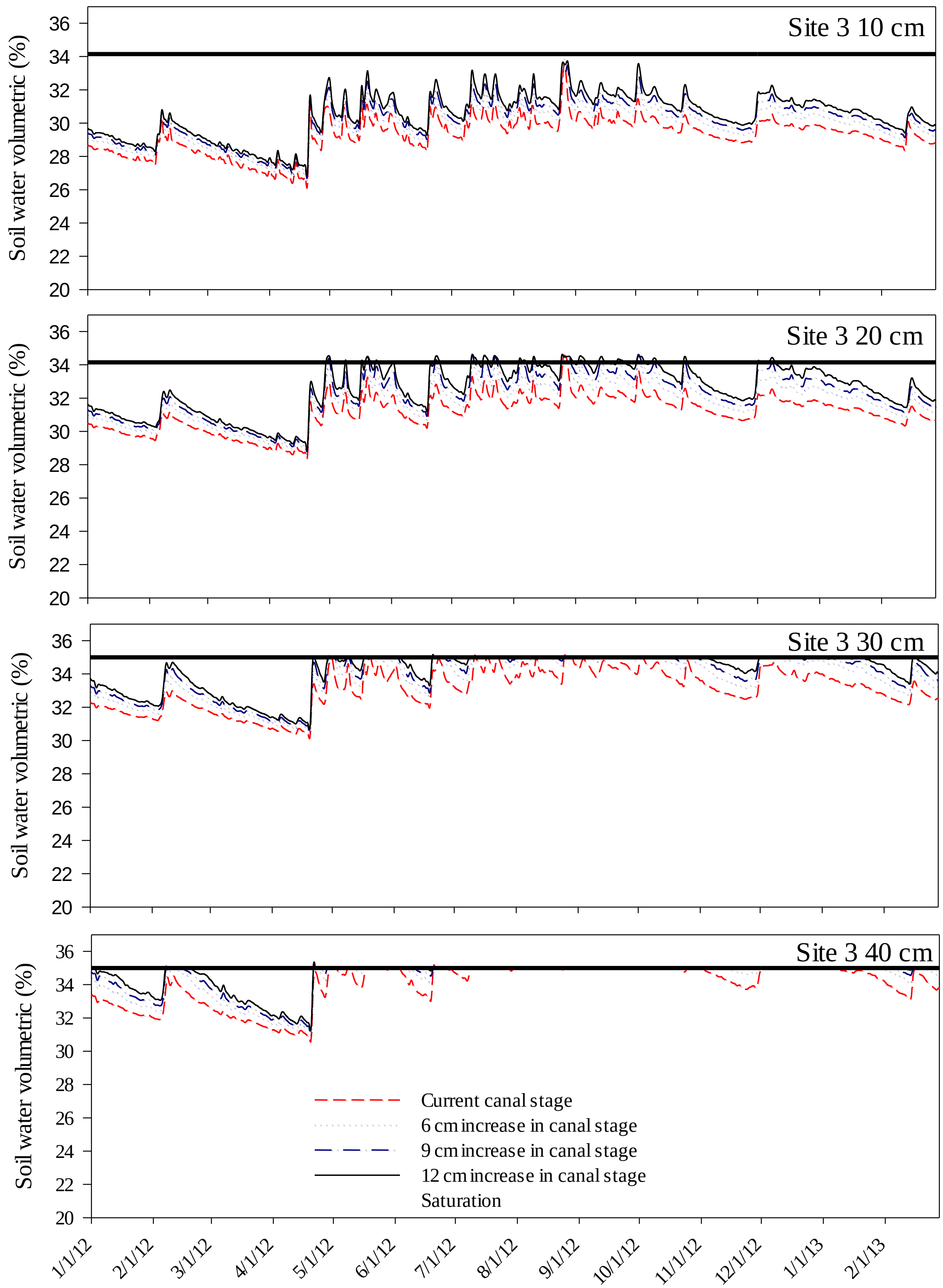

Figure 10. Simulated volumetric soil water content under different C-111 canal stage management scenarios at four different depth at site 3[caution: absolute predictions should be

regarded as qualitative assessments only due to uncertainty in measured data used in developing the model].

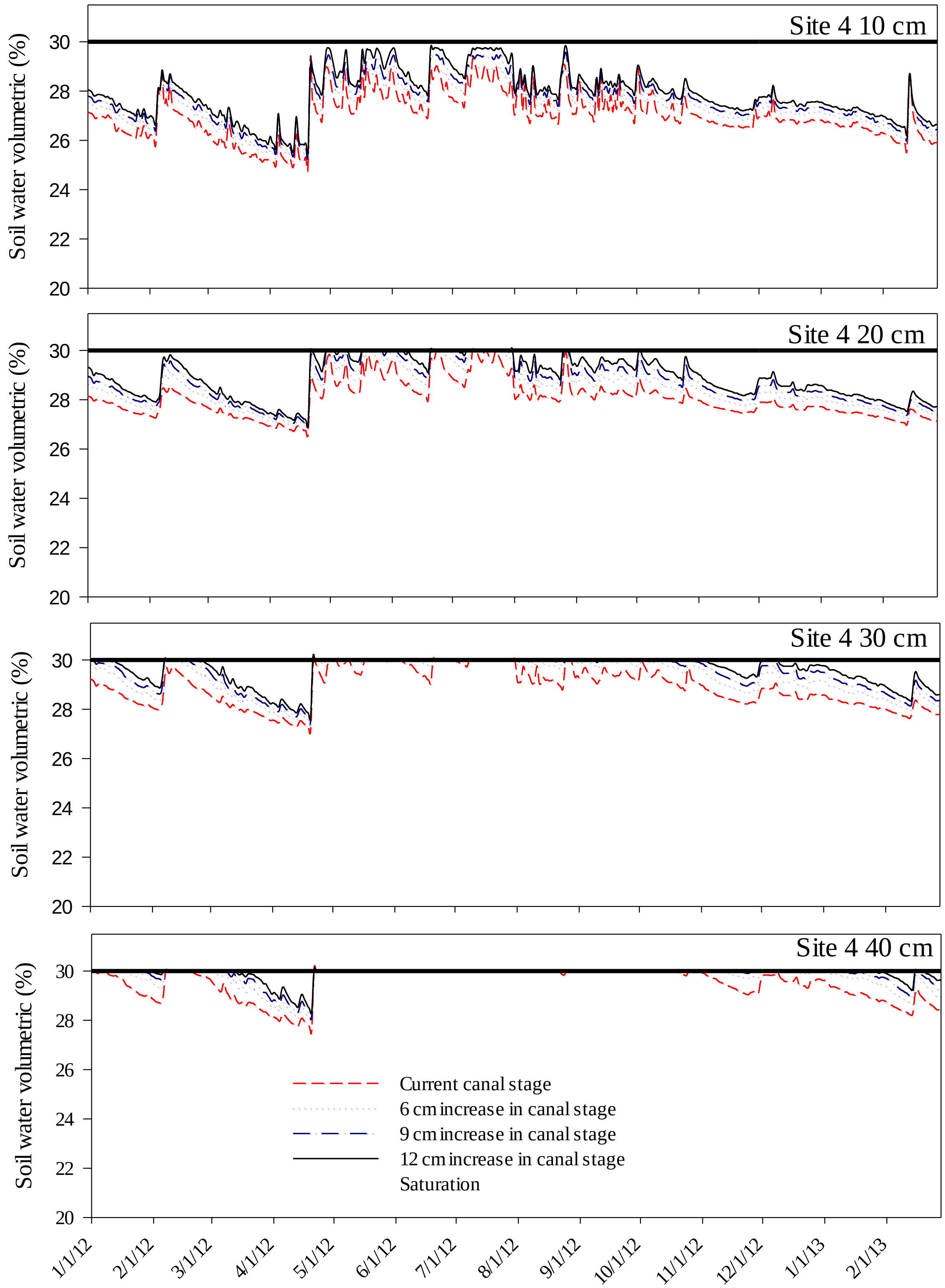

Figure 11. Simulated volumetric soil water content under different C-111 canal stage management scenarios at four different depth at site 4[caution: absolute predictions should be regarded as qualitative assessments only due to uncertainty in measured data used in developing the model].